SynLight: Synthetic Light Emission for Fast Transmission in COTS Device-enabled VLC

Yanbing Yang[1,2] Jun Luo[2] Chen Chen[3,4] Wen-De Zhong[4] Liangyin Chen[1]
[1]College of Computer Science/Institute for Industrial Internet Research, Sichuan University, P.R. China
[2]School of Computer Science and Engineering, Nanyang Technological University, Singapore
[3]School of Microelectronics and Communication Engineering, Chongqing University, P.R. China
[4]School of Electrical and Electronic Engineering, Nanyang Technological University, Singapore
Email: {yangyanbing, chenliangyin}@scu.edu.cn, {junluo, chen0884, ewdzhong}@ntu.edu.sg

***Abstract*—*Visible Light Communication* (VLC) systems relying on commercial-off-the-shelf (COTS) devices have gathered momentum recently, due to the pervasive adoption of LED lighting and mobile devices. However, the achievable throughput by such practical systems is still several orders below those claimed by controlled experiments with specialized devices. In this paper, we engineer SynLight aiming to significantly improve the data rate of a practical VLC system. SynLight adopts COTS LEDs as its transmitter, but it innovates in its simple yet delicate driver circuit wiring an array of LED chips in a combinatorial manner. Consequently, modulated signals can directly drive the on-off procedures of individual chip groups, so that the spatially synthesized light emissions exhibit a varying luminance following exactly the modulation symbols. To obtain a readily usable receiver, SynLight interfaces a COTS Photo-Diode with a smartphone through the audio jack. The evaluations on SynLight are both promising and informative: they demonstrate a throughput up to 60 kbps, more than 50× of that achieved by state-of-the-art systems, while suggesting various potentials to further enhance the performance.**

I. Introduction

Visible Light Communication (VLC) has long been envisioned as an alternative to RF communications, and it keeps attracting attentions given the increasing scarcity of RF spectrum resources. In the past decade, experimental VLC setups with highly sophisticated constructions have been able to deliver a throughput up to a few Gbps [1], yet none of them have been put into practice by far. At the meantime, practical VLC systems relying on commercial-off-the-shelf (COTS) devices have been gaining their momentum, mainly thanks to the pervasive adoption of *Light Emitting Diodes* (LEDs) lighting [2] and mobile devices (e.g., smartphones). Whereas these practical developments admit immediate deployments, the achieved throughput, only at kbps level (e.g., [3], [4], [5]), is far below that claimed by the experimental setups. Fortunately, we believe that there is a big potential to close the gap between practical and experimental systems.

To our understanding, one major reason that prevents those high-performance experimental setups from becoming practical is the nonlinear nature of LEDs [6], [7]. Essentially, the relation between LED input (voltage or current) and output (intensity or luminance) can be highly nonlinear, and this distortion is affected by LED types and ambient conditions (e.g., temperature) as well. Existing solutions overcome this nonlinearity by either sacrificing spectral efficiency or applying complicated processing logic or circuits [8], [9]. While the former method (already adopted by practical VLC systems) yields simple but inefficient modulations (e.g., OOK [10] or PPM [11]) that largely confine the throughput, the latter significantly increases the system complexity and hence reduces the robustness to, for example, ambient noises and interferences, making its feasibility very questionable in practice.

Another obstacle to deploy high-performance VLC setups is their high costs. These experimental setups always utilize high-power LEDs and high-sensitivity *Photo-Diodes* (PDs), and they may also apply special lenses and filters [1], [12]; all these imply a high cost. In reality, VLC has certain obvious drawbacks: it is directional and requires *Line-of-Sight* (LoS) links thus cannot provide a sufficient coverage as WiFi does, and it is invasive as light emissions with a high intensity can be very disturbing to human users. As a result, a reasonable choice of VLC transmitters would be the existing (or at least upgraded) lighting infrastructure, rather than any specifically designed modules similar to the WiFi access points. In the context of piggybacking on a lighting infrastructure, the cost incurred by high-performance VLC setups appears prohibitively high, and some of the incurred complications (e.g., lenses and filters) simply become inapplicable.

Unfortunately, recently proposed practical VLC systems are all too conservative in addressing aforementioned challenges [5], [13], [14], [15], [16], [17], resulting in a throughput only up to a few kbps. They mostly resort to low-order modulations that trade spectral efficiency for avoiding nonlinearity, and they exploit the rolling-shutter effect of cameras (readily usable for all smartphones but badly performing in frequency response) to suppress the system complexity. Color-Shift Keying [15] is a high-order modulation inspired by Wavelength-Division Multiplexing, yet introducing colorful LED luminaires largely confines its practicality on common white LED lighting infrastructure. ReflexCode [5] slightly increases the modulation order at the cost of involving multiple LED luminaires, which may confine the system applicability.

This work was supported in part by the Fundamental Research Funds for the central Universities, National Natural Science Foundation of China under Grant No. 61373091, the AcRF Tier 2 Grant MOE2016-T2-2-022, and the DSAIR Center at NTU.

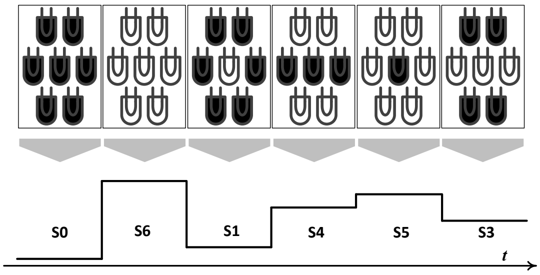

Fig. 1. The idea of synthetic light emissions: the emissions from multiple LEDs are controlled so that the spatially synthesized intensities represent respective modulation symbols.

Apparently, more aggressive designs are key to close the gap between practical deployments and experimental setups.

To this end, we design SynLight to probe the limit of COTS VLC systems from both transmitter and receiver sides. To enable higher-order modulations given the LED nonlinearity, we revisit the idea of spatial synthesizing for intensity modulation [18], but we innovate in a compact circuit design that generates up to 256-PAM (*Pulse Amplitude Modulation*) with a COTS LED array. Essentially, the transmitter of SynLight wires an array of LED chips in a combinatorial manner and directly drives the on-off procedures of individual chip groups according to the modulation symbols. As a result, the signal patterns get linearly "translated" to varying luminance, thanks to the spatially synthesized light emissions, as shown in Fig. 1. In order to relax the bottleneck at CMOS cameras while still maintain practicality (i.e., the ability of using smartphones as receivers), we adopt an approach to interface a PD with a smartphone: a plug-in solution via the audio jack. In summary, we make the following major contributions:

- A novel transmitter built upon COTS LEDs to generate high-order modulations (up to 256-PAM) without being troubled by LED nonlinearity.
- A calibration scheme to automatically handle the LED chip diversity in transmitter production.
- A practical receiver interfacing a PD with a smartphone through the audio jack, and achieving a high-speed transmission via specially designed coding/decoding schemes.
- Extensive evaluations with SynLight prototype to not only demonstrate its promising performance but also provide guidelines for future developments.

SynLight is not meant to chase the best performance, but rather aims to explore different aspects of realizing COTS-enabled VLC in practice. It provides us with a better understanding of potentials and limits of the COTS VLC systems in general. In the following, we first introduce the background in Section II. The transmitter and receiver of SynLight are then presented in Section III and IV, respectively. We further report and discuss the extensive evaluations in Section V and finally conclude our paper in Section VI.

II. Preliminary and Motivation

We set up the background for developing SynLight in this section. We first briefly explain the LED nonlinearity and the potential solution based on spatial light synthesizing. Then we study the performance of COTS LED in terms of frequency response, for both single LED chip and chip groups. We finally discuss the challenge of interfacing a PD with smartphones.

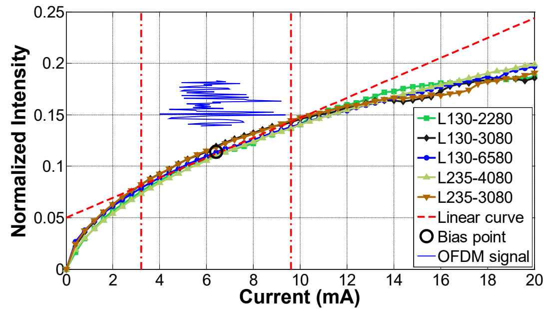

Fig. 2. LED Nonlinearity.

A. Nonlinearity of LED

It is well known that an LED has strong nonlinearity [6], [7], making it very hard to realize high-order modulations. Most proposals confine the (luminance) dynamic range of LEDs to a very narrow section so as to retain linearity [1], [19] (the OFDM signal shown in Fig. 2), but they require a very high transmitting power or special lens/filters to achieve an adequate *Signal-to-Noise Ratio* (SNR) at the receiver. This method is obviously not feasible for COTS VLC piggy-backing on an existing light infrastructure subject to certain luminance control. Other proposals resort to predistortion or postdistortion [8], [9] to rectify the nonlinearity, they yet require complicated processing circuits, and even worse, these circuits have to be fine-tuned to suit individual LEDs given their different manifestations of nonlinearity. Fig. 2 shows a few typical LED input response curves that are measured based on several types of LEDs chips (with different color temperatures); The nonlinearity and its varying manifestations with different LED types are quite evident.

Alternatively, varying luminance (thus realizing intensity modulations) can be made effective by spatially synthesizing the light emissions from a group of LEDs with a varying size [20]. Under this method, individual LEDs only experience an On-Off process like OOK so that nonlinearity does not matter at all. However, existing implementations all stay at small scales and mostly apply high power LEDs, with only channel quality measurements that are of little practical significance [20], [21]. In Section III, we will present our transmitter prototype based on the same principle but enabling full-fledged data transmissions, but before that, we need to understand the performance of COTS LEDs under high frequencies, especially when they are grouped.

B. Frequency Response of Single LEDs

In order to control the On-Off process of LED chips, existing LED luminaires have to be upgraded so that control signals can be exerted on individual chips. In this section, we test the frequency response of the COTS illumination LEDs controlled by low-cost transistors[1]. We use a function

[1]We use the extremely low-cost (0.06 USD per chip) and small-size transistor MMSS8050-H-TP, in order to suppress the potential cost for upgrading LED luminaires.

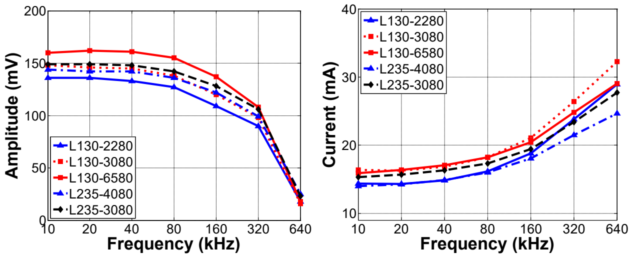

(a) Recv. light intensity. (b) Driving current.

Fig. 3. Frequency response of single LEDs. (a) Received light intensity decreases with frequency, while (b) driving current increases.

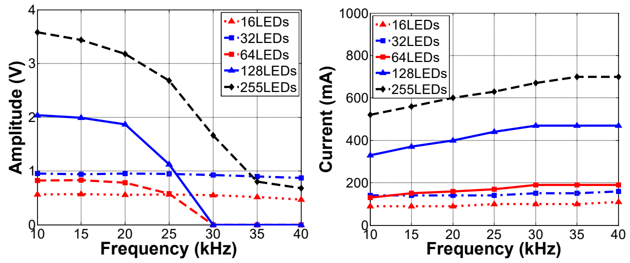

(a) Recv. light intensity. (b) Driving current.

Fig. 4. Frequency response degradation caused by grouped LEDs.

generator to generate OOK signals with the frequency varying from 10 kHz to 640 kHz to drive the LEDs, and we report the received light intensity by PDA10A without any filters in Fig. 3(a). We also investigate the performance by various types of LEDs with different color temperatures, ranging from 2200 K (warm white) to 6500 K (cool white). We observe that color temperature does not have a major impact, and the cut-off frequency at around 320 kHz is evident. This limit is set by the phosphor coating used for COTS illuminating LEDs [22]: though LED chips usually have a relatively fast switching speed, they are slowed down by that of the phosphor coating. Moreover, we employ a multimeter to measure the average DC current consumed by the LEDs and plot the outcome in Fig. 3(b). It is intuitive to observe that a higher frequency increases the power consumption due to the LED's parasitics. Both results suggest that chasing a higher throughput by increasing frequency may not be efficient for COTS illumination LEDs, motivating us to target at higher-order modulations.

C. Grouping Degrades Performance

Implementing spatially light synthesizing by controlling individual LED chips may cause an over-complicated driver circuit, but grouping the chips wisely can significantly reduce the driver complexity. For example, controlling 7 chips to obtain 8 levels of luminance only requires 3 control signals (rather than 7) if the chips are put into 3 groups with sizes 4, 2, 1, respectively. However, the performance bottleneck now becomes the largest group, because all chips in it are controlled by one transistor and an isolator is needed to protect the MCU from the high voltage control signal.

Here we test the frequency response of LED groups under typical cascade and parallel connections used by SynLight transmitter detailed in Section III. The same transistor is

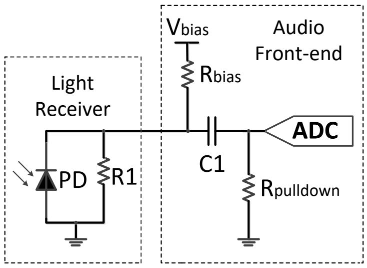

Fig. 5. Circuit diagram of a VLC receiver via smartphone audio jack, including a model of the audio front-end and a photodiode receiver.

used for the control purpose and a low-cost isolator TLP293-4 is put between the MCU and driver. Fig. 4 reports the experiment results given the same metrics used for Fig. 3. The drastic reduction in working frequency (compared with single LEDs measured in Section II-B) mostly attributes to the low-cost isolator. Also, the saturation of the transistor limits the driving current and hence the input power. Consequently, the overall low-cost design of SynLight allows for a safe working frequency up to 25 kHz. Obviously, replacing the transistor and isolator with their high-performance (thus high-cost) counterparts would increase this frequency, but this is out of the scope of our SynLight objective, which aims to exploit higher-order modulations for improving spectral efficiency.

D. Audio Jack as VLC Receiver

An ideal COTS VLC receiver should be integrated into smartphones (like the WiFi module). While such an integrated design is desirable, we need a receiver immediately applicable to smartphones, which naturally leads to the adoption of audio jack. Using audio jack as a VLC receiver is not new, but existing proposals only support a very low throughput, e.g., 0.7kbps reported in [23]. Fig. 5 shows a typical VLC receiver based on audio jack. The internal bias voltage drives the reception

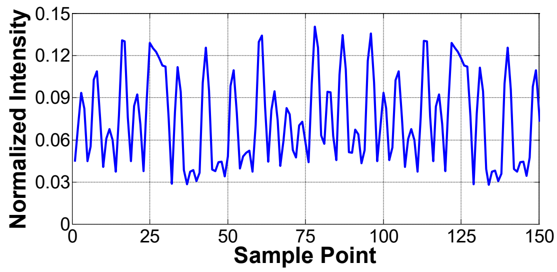

(a) Data sampled by phone's audio interface.

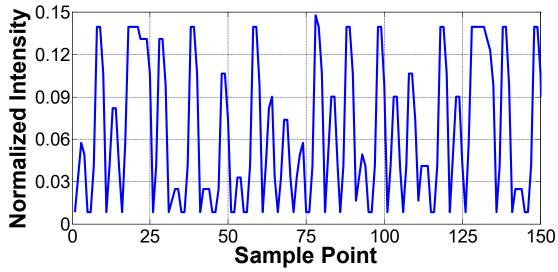

(b) Data sampled by a digital oscilloscope.

Fig. 6. Sampled signals by the smartphone's audio interface comparing with those sampled by a digital oscilloscope.

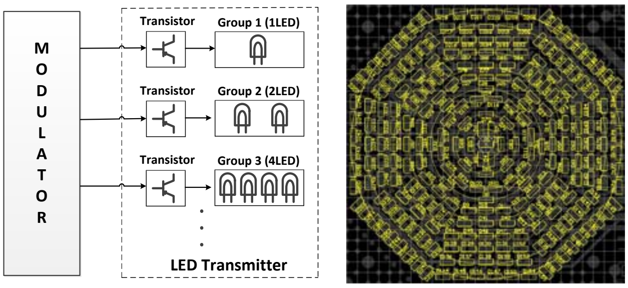

(a) The combinatorial grouping of LED chips.

(b) Layout of 255 LED chips.

Fig. 7. The front-end of SynLight transmitter.

circuit with a photodiode and parallel resistor, allowing the ADC directly acquires the analog signals generated by the receiver and making it seemingly straightforward to act as a plug-and-play receiver [23], [24], [25].

However, the coupling capacitor, i.e., C1 in Fig. 5, limits the DC component of input signal hence strongly affecting the performance of amplitude-based high-order modulation schemes such as PAM. Fig. 6 graphically compares the signal sampled from the audio interface with that sampled by a digital oscilloscope at similar sample rates: 44.1 kHz for the former and 50 kHz for the latter. Apparently, the signal distortion caused by audio sampling can seriously affect on the demodulation performance. Therefore, SynLight requires a new coding/decoding scheme to mitigate this distortion.

III. SynLight Transmitter

In this section, we detail the theoretical analysis, design and implementation of SynLight transmitter.

A. *Front-end with Reduced Control*

As mentioned in Sec. II-A, exerting control on individual LED chips can unnecessarily increase the driver complexity. Therefore, we wire the chips in a combinatorial manner, i.e., we group them so that the output optical power grows in a stepping manner of a power of two, as shown in Fig. 7(a). As a result, an LED array with N chips only requires $\log N$ control signals. Moreover, such an arrangement leads to a natural "translation" from digital bits to modulation intensities. For example, the first group (containing only one chip) is driven by the least significant bit of one byte (assuming 255 chips in the array to be driven by a *codebook* containing one byte control codes), and the most significant bit drives the last group with 128 chips. The physical layout of the LED chips in our SynLight prototype is illustrated in Fig. 7(b), where we choose an octagon shape to emulate a common LED luminaire[2] with a disk face, and we symmetrically place the first group at the center and the last group at the periphery.

B. *Synthetic Light Emissions*

We study the performance of spatial light synthesizing through both modeling and experiments. Fig. 8 illustrates the principle of spatial synthesizing of K_i LED chips in a group.

[2]This is partially inspired by the lighting infrastructure used in our institute, where each $16\,\text{m}^2$ office is lit by four LED luminaires each with 288 chips.

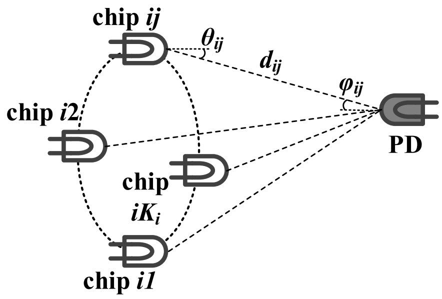

Fig. 8. Modeling the synthetic light emissions from the i-th group containing K_i LED chips.

Following the common practice [26], we assume that the emission of each chip follows a Lambertian radiation pattern. Considering only the LoS component and without using the optical filter and lens, the optical channel DC gain between the j-th chip of the i-th group and the PD is calculated as

$$h_{ij} = \frac{(m+1)A}{2\pi d_{ij}^2}\cos^m(\theta_{ij})\cos(\varphi_{ij}), \tag{1}$$

where m is the Lambertian emission order given by $m = -\ln 2/\ln(\cos(\Theta))$ with Θ being the semi-angle at half power of each chip, A is the active area of the PD, d_{ij} is the transmission distance between the chip and the PD, θ_{ij} and φ_{ij} are the emission angle and the incident angle, respectively. If the incident light is outside the field-of-view of the receiver, the corresponding channel gain becomes zero.

In the proposed synthetic light emissions, all the LED chips have only two states, i.e., On and Off, so we have a binary control process $x_{ij}(t) \in \{0, 1\}$ for each chip. Assuming that a total of G groups of LEDs are used, the overall spatially synthesized light intensity at the PD can be obtained by

$$y(t) = \textstyle\sum_{i=1}^{G}\sum_{j=1}^{K_i} R h_{ij} x_{ij}(t) + n(t), \tag{2}$$

where R is the responsivity of the PD and $n(t)$ is the corresponding additive thermal and shot noises. The additive nature of Eqn. (2) confirms that the synthetic effect of multiple On-Off control processes should lead to a linear increase in *Received Light Intensities* (RLIs), which is key to SynLight and is shown as the theoretical curve in Fig. 9. However, due to the component diversity and particular circuit configurations, the actually measured RLIs are not exactly linear, as shown in Fig. 9. Essentially, as individual LED chips may not be

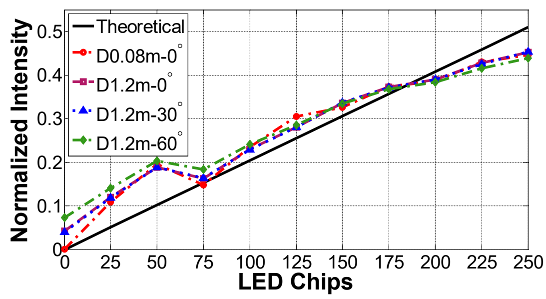

Fig. 9. Normalized RLIs: theoretical analysis and experiment measurements. We measure the RLIs at two distances (0.08 m and 1.2 m) and also three view angles at the longer distance. The differences between the analysis and measurements are mainly due to component diversity and circuit configurations.

uniform in their output optical intensities, the overall RLIs start to deviate from the ideal linearity when various groups of chips are involved.

C. Adaptively Calibrated Emissions

Due to the chip diversity in production, the synthetic light intensity is not strictly linear with the number of alight LED chips as shown in Fig. 9. Conventionally, we may fine-tune the driver circuit to rectify this[3], but such a method is no difference from the predistortion applied to counter the inherent LED nonlinearity (see Section II-A), i.e., every produced transmitter has to be manually calibrated, which is too cumbersome to meet the need for constructing large scale VLC systems in practice. A practical calibration method should solely rely on adjustments on the software side.

Taking the advantage of SynLight's stepping power control ability, we propose an adaptive calibration to rectify the non-linearity by only adjusting the modulation codebook. Given the original codebook $\boldsymbol{C}^{\mathrm{PAM}}$, the element c_i^{PAM}, where the subscript i refers to the i-th modulation symbol, is set to $\lfloor 255 \times i/M \rfloor$ initially, with M denoting the modulation order. We let the transmitter step up the number of On chips from 0 to N (where N denotes the total number of chips), and we record the corresponding RLIs shown in Fig. 10(a) as "original". The recorded light intensities are stored in a vector

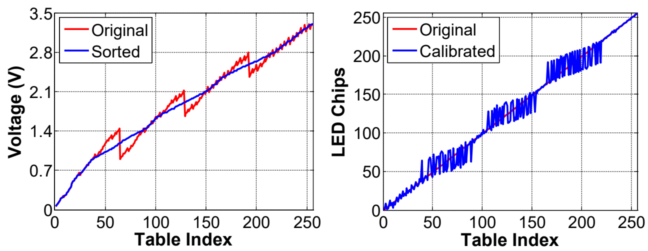

(a) RLIs before/after sorting. (b) Codebook calibration.

Fig. 10. Adaptive calibration based on RLIs.

$\boldsymbol{\ell} = [\ell_0, \ell_1, \cdots, \ell_N]$, and the corresponding control code c_i is set in the codebook as $c_i = i$ assuming the system is linear. Now we sort $\boldsymbol{\ell}$ ascendingly and adjust the corresponding codes in the codebook $\boldsymbol{C}$: i.e., if ℓ_i and ℓ_j exchanged their positions after sorting, the value of c_i and c_j should also be exchanged. Finally, we go through the original codebook $\boldsymbol{C}^{\mathrm{PAM}}$ ascendingly and look up in the sorted $\boldsymbol{\ell}$ for the one ℓ_k that best represents c_i^{PAM} (using the expected light intensity $\tilde{\ell}_i$ as a reference and $\epsilon > 0$ as the error threshold), and we update the code c_i^{PAM} using the value of c_k. We illustrate the outcome in Fig. 10(b).

In Fig. 11, we use the calibrated 8-PAM as an example. According to Fig. 11(a), the RLIs are perfectly linear with respect to the PAM symbols after our calibration. The differences shown in Fig. 11(b) between expected codes and the adjusted codes clearly demonstrate the effect of calibration. For example, the symbol S3 (binary value 011) is expected to be produced by alighting 110 chips (corresponding to

[3]Existing proposal [20] applies a current-limiting resistor to every chip group so as to enable the fine-tuning.

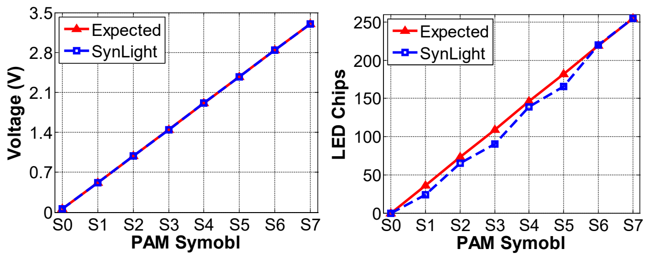

(a) 8-PAM symbols vs. RLIs. (b) 8-PAM symbols vs. codes.

Fig. 11. Adaptively generated 8-PAM symbols using the calibrated codebook.

code 01101110), but the transmitter actually alights 90 chips (code 01011010) to retain the linearity after calibration. Note that this calibration procedure, with an assistance of a high-quality PD (we use PDA36A [27]), is fully automated without the need for human intervention, so it is totally suitable for massive production.

D. From Message to Modulated Light

In a typical unidirectional VLC system, messages are firstly coded by *Forward Error Correction* (FEC) codes into encoded packets to combat the packet loss. Subsequently, the encoded packets are modulated into control codes to drive the LED front-end, so as to embed digital information onto light intensity. We briefly illustrate the procedure of embedding messages into modulated light in Fig. 12(a). Moreover, VLC is considered as a secondary functionality piggybacking on a modern LED lighting infrastructure (as discussed in Section I), so the proposed VLC transmitter should avoid causing any visible flicker during data transmissions.

SynLight applies 4B6B *Run Length Limit* (RLL) line coding for its simplicity and DC balance [28]. 4B6B coding generates

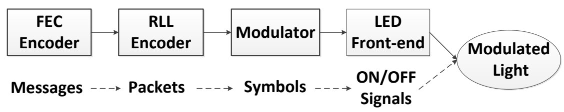

(a) A message is encoded and modulated to be sent via light.

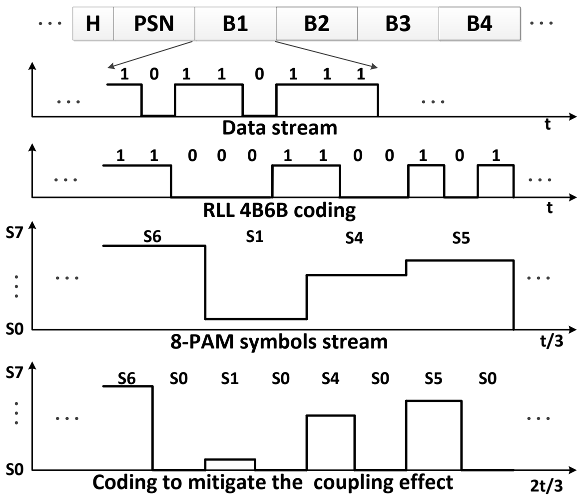

(b) An FEC encoded packet is further encoded with RLL 4B6B and then modulated with 8-PAM.

Fig. 12. Diagrams of coding/modulation procedures for SynLight transmitter.

6 encoded bits for each 4 data bits while maintaining no more than three successive “1” or “0”, meaning that a half data byte (4 bits) require two 8-PAM symbols or one 64-PAM symbol. Under 8-PAM, a byte coded with 4B6B thus requires 4 symbols as shown in Fig. 12(b) (we refer to Table 4 in [28] for the 4B6B mapping). More detailed studies show that combining 4B6B with 8-PAM ends up with only 6 useful symbols (S1 to S6); a phenomenon occurs similarly to all 2^k-PAMs with an odd k. Therefore, we can reduce 8-PAM scheme to 6- or 7-PAM[4] scheme that represents the same amount of information with less symbols. This reduced modulation scheme benefits SNR because of less light intensity steps within the same output range. In other words, we may increase the symbol distance to improve the signal strength and thus the data rate.

E. Coding for AC Coupling

As mentioned in Section II-D, using the audio jack of a smartphone as a VLC receiver demands a special coding scheme to combat the signal distortion caused by the special construction of the audio front-end. Specifically, AC coupling could interfere modulated signals due to the coupling capacitor filtering the DC component, but amplitude-based modulation suffers the most as it requires the circuit output to maintain a stable amplitude from time to time. To mitigate the AC coupling effect caused by the capacitor, we propose a new coding based on 4B6B before modulation. The lowest part in Fig. 12(b) shows the designed coding: each significant symbol is followed by a S0 to convert any DC “plateau” to an AC falling edge, and adding S0 causes the sharpest edge possible under unipolar VLC. With this novel coding scheme, a SynLight receiver can avoid measuring the absolute amplitude value easily distorted by the AC coupling; it may instead detect the amplitude difference between any two adjacent symbols. Detailed decoding procedure is presented in Section IV.

IV. SynLight Receiver

As the receiver from a practical VLC system, we would like it to be readily applicable to smartphones (the most pervasively used COTS mobile devices). However, high-speed communication modules need to be integrated into a phone, which is certainly beyond our reach. Therefore, we interface a low-end PD to the phone’s audio jack, confirming the readily usable nature of SynLight.

A. Packet Extraction via Header

As mentioned in Section III-D, modulated light emissions carry encoded messages. The receiver uses a PD to sense these emissions and converts them to voltage signals sampled by the audio interface of a smartphone. As VLC is asynchronous and one-way, each data packet contains a header to indicate the start of valid data transmissions. The receiver then recognizes

[4]Though 6-PAM is already sufficient, SynLight has to adopt a different coding scheme for the audio receiver explained in Section III-E. So we actually use 7-PAM for SynLight prototype, but still name “8-PAM” in evaluation part for technical expression.

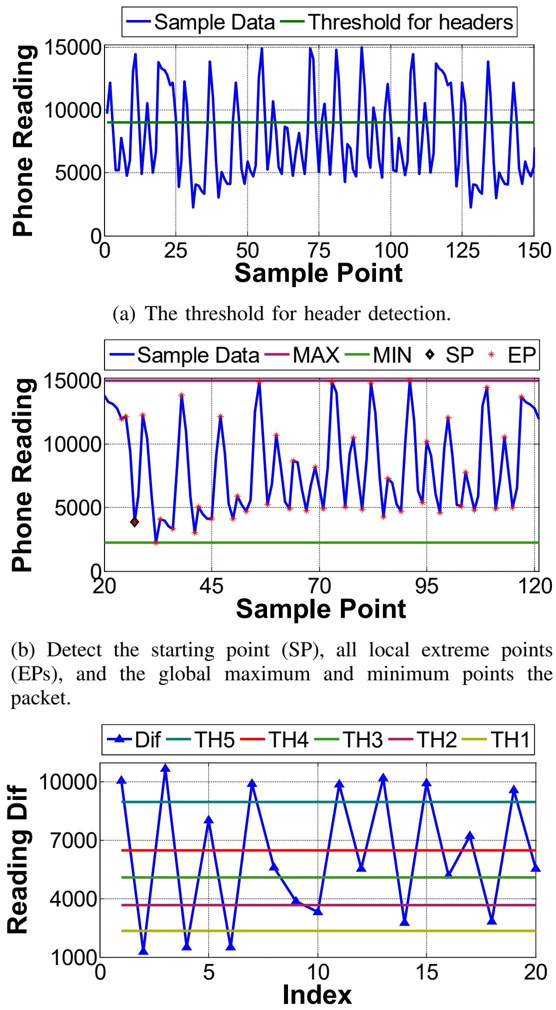

(a) The threshold for header detection.

(b) Detect the starting point (SP), all local extreme points (EPs), and the global maximum and minimum points the packet.

(c) Thresholds for symbol detection exploiting the differences between pairs of local maximum and minimum.

Fig. 13. SynLight demodulation procedure.

data transmissions by detecting the headers. As shown in Fig. 13(a), a valid header has a relatively high light intensity and holds on for the longest time; we refer to Section V-A for more details on packet format. Before decoding, SynLight uses the first few samples (typically 200) to search for the maximum value of sampled data. Then it sets a rough threshold based on this maximum; this threshold, along with a typical duration, are used to detect headers. Here we empirically configure the 0.6 of the maximum value as the threshold to maximize the chances of detecting headers.

B. Demodulation with Differential

Once two adjacent headers are recognized, the demodulator starts examining the samples between the two headers with a window determined by the transmission frequency and sample rate. The demodulation procedure is triggered by the first minimum value point in the packet right after the header (SP marked by a black $\diamond$ in Fig. 13(b)). Meanwhile, SynLight detects all extreme points (i.e., local maximum and minimum points, EP marked by red $*$ in Fig. 13(b)) via the first order differences of the samples, as the first order differences cross zero around all extreme point. Two neighboring extreme points are then paired to derive the absolute difference in values (blue ▲) as shown in Fig. 13(c). According to the coding scheme described in Section III-E, a local maximum represents a PAM symbol and a subsequent local minimum is the artificial zero created by our coding scheme to remove the DC component, so the difference between them indicates the symbol value. Moreover, we use the absolute difference between the global maximum and minimum in the packet, shown in Fig. 13(b) by two baselines, to proportionally configure thresholds for symbol detections. Once all symbols in the packet are recognized, the resulting candidate packet is then given to the FEC decoding for recovering the original message.

V. Evaluations and Discussions

We extensively evaluate the performance of SynLight in this section, mainly in its real-life communication capacity. Based on the experiment results, we also seriously discuss the potentials and limits of SynLight, aiming to seek out potential methods for further improving the data rate of practical VLC.

A. Experiment Settings

Transmitter: We build SynLight's transmitter that integrates COTS components onto a 4-layer PCB with a size of 10 cm × 7 cm as shown in Fig. 14. As already explained in Section III-A, the transmitter front-end consists of 255 LED chips divided into 8 groups, and the i-th group has 2^i LED chips with $i = 0, 1, \cdots, 7$. The COTS illumination LED chip LUXEON 3014 ($ 0.26 per chip) is adopted to form this transmitter front-end. We employ a low-cost MSP430F2618 MCU as the controller to generate control signal for modulation. Two very low-cost 4-ch TLP293 optocouplers ($ 1.18 each) are used to isolate the high voltage control signals from the MCU. Each LED group is directly controlled by one or more low-cost MMSS8050 transistors ($0.06 each). As the maximum driving current of MMSS8050 is 1.5A, a single transistor may support only up to 16 LED chips in a group. So we need to use multiple transistors in parallel for groups with more than 16 chips to maintain a current below 1.5A for each transistor.

Receiver: We use a PD SD3421 as the receiver front-end due to its wide FoV suitable for practical applications, and employ a Nexus 6 as the host to the front-end. As illustrated in Fig. 5, we use an audio plug to directly connect the PD to the phone's audio jack so as to leverage the ADC and processors of the phone. The sample rate is configured at 44.1 kHz.

System configuration: We define each packet as containing a 4 bytes payload and identified by an 8-bit *Packet Sequence Number* (PSN), and all these are led by a header of 1 lowest symbol (S0) and 3 successive highest symbols (e.g., S7 for 8-PAM), as shown in Fig. 12(b) (the top). Since VLC is asynchronous and one-way, we employ a FEC scheme of Raptor coding to encode the message, and the coding overhead is set as 25%. Moreover, we adopt RLL 4B6B to avoid flicker of the LED front-end, as discussed in Section III-D. To further handle the AC coupling of the audio interface[5], the new coding scheme proposed in Section III-E is applied on the transmitter side. The transmission power is set to obtain an intensity of 400 lux at 1.2 m. Each of our following experiments consists of 10 sessions and 320 packets (before FEC) are transmitted within each session. We report the average values over all sessions, except for data rates whose maximum values are also reported.

Fig. 14. SynLight's transmitter (left) and receiver (right).

B. Channel Property under PAM

In this section, we study the performance of SynLight's high-order modulations given different experimental settings.

1) Transmission Frequency: The operating frequency of the transmitter is the most important parameter that affects the data rate, so we first study its impact on the VLC channel quality, and we report the *Packet Error Rate* (PER) for the designed receiver under various transmission frequency in Fig. 15(a). Here we position the receiver at a distance of 40 cm from the transmitter. We vary the frequency from 10 kHz to 25 kHz. The relatively low transmission frequency is confined by the transmitter's feasible frequency studied in Section II-C and the receiver's sample rate. Although SynLight's transmitter is able to generate up to 256-PAM, the decreasing symbol distance makes it very hard to demodulate the signals beyond 8-PAM at a reasonable distance. As reported in Fig. 15(a), SynLight's receiver can only support a frequency up to 20 kHz given its sample rate at 44.1 kHz. In the following, we hence fix a transmission frequency of 20 kHz.

2) Distance and View Angle: We also evaluate PERs of 4-PAM and 8-PAM with respect to both communication distance and (receiver) view angle; the results are reported in Fig. 15(b) and 15(c), respectively. We vary the distance from 30 cm to 80 cm. It is quite clear that increasing the distance degrades the demodulation performance yet it can still support a distance up to 70 cm for both two modulation schemes of 4- and 8-PAM. Moreover, it is feasible to largely extend the communication distance with an amplifier powered by harvesting the energy from audio jack as done in [24], but we leave it as a future work on our schedule. Setting the communication distance as 40 cm, we further examine the PER by changing the viewing angle within $[-30, 30]^\circ$ for the receiver. Agreed with the results discussed in Section III-B, changing the viewing angle within 30° barely affects the channel quality as shown in Fig. 15(c), thanks to the wide FoV of both PDs and COTS illumination LEDs adopted by SynLight. Should we add a lens to focus the light emissions so as to improve the channel quality at around 0° (like most experimental settings achieving

[5]The AC coupling can naturally filter the interference caused by ambient light variance, we hence skip evaluations for ambient light in this paper.

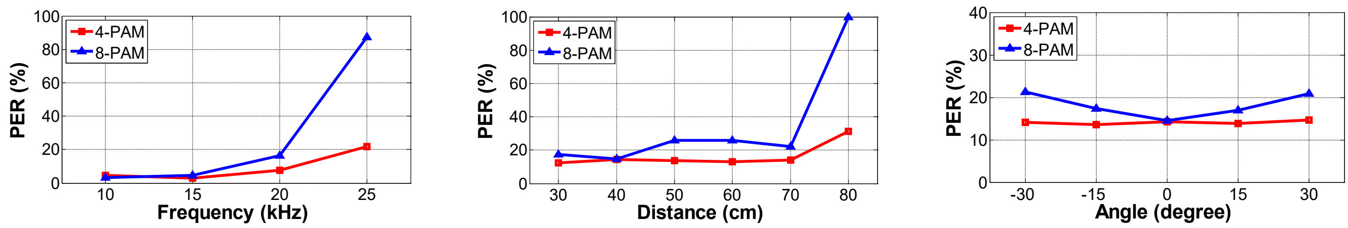

(a) Varying transmission frequency. (b) Varying transmission distance. (c) Varying receiver's viewing angle.

Fig. 15. PER under different experiment settings.

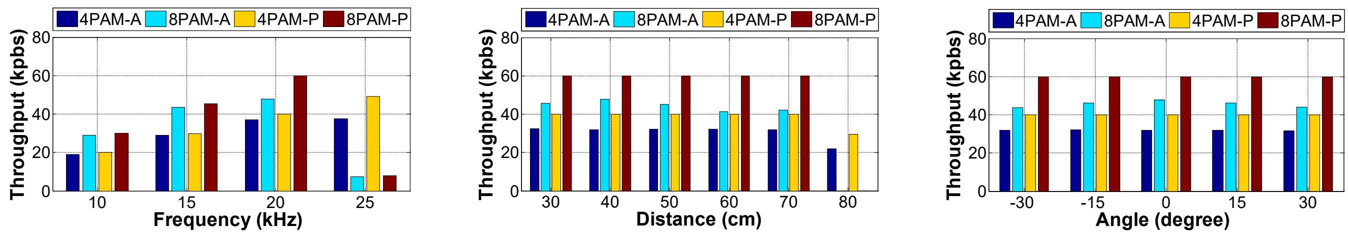

(a) Throughput vs. transmission frequency. (b) Throughput vs. communication distance. (c) Throughput vs. viewing angle.

Fig. 16. Throughput under various experiment settings.

very high data rates), the channel quality would be drastically degraded at other angles. Although 4-PAM has slightly lower PERs than 8-PAM thanks to its larger symbol distance under all tests, it may still be worth of using 8-PAM given its higher bit-symbol-ratio.

C. Throughput Evaluations

In this section, we report the achievable data rates by SynLight under various experiment settings.

1) Transmission Frequency: Within a reasonable frequency range studied in Section V-B, the data rate of SynLight heavily depends on transmission frequency. As shown in Fig. 16(a), the achieved throughput of SynLight increases almost linearly with the transmission frequency, as every hertz carries a PAM symbol. In accordance with the observations made in Section V-B1 (where the same distance settings are taken), 4-PAM appears to be a more stable as the variance in throughput is small, whereas 8-PAM has a much higher peak rate in most cases, except when the frequency goes beyond the safe range (e.g., 20 kHz). In particular, SynLight's receiver achieves a maximum throughput up to 60kbps (and an average of 40kbps) with 8-PAM at a frequency of 20 kHz.

2) Distance and View Angle: We now verify the data rate of SynLight from the application perspective, namely at varying distances and viewing angles. The throughput provided by SynLight generally degrades with an increasing distance as shown in Fig. 16(b), and a simple PD without amplifier seems to have a threshold that throttles the performance of the receiver beyond 70 cm, but it is feasible to enlarge the communication range by using an amplifier as mentioned in Section V-B2. Nevertheless, SynLight still reaches a peak throughput up to 60 kbps (with an average value beyond 40 kbps) at 70 cm with 8-PAM as reported in Fig. 16(b); this is more than 50× of that (0.7 kbps at 40 cm) reported in [23]. As one may expect given the channel quality results in Section V-B2, changing receiver's viewing angle does not significantly affect on throughput as depicted in Fig. 16(c). All these results strongly confirm the robustness of SynLight under real-life application scenarios.

D. Potentials and Limits: A Discussion

Receiver: Although SynLight suppresses the LED nonlinearity and can in principle reach up to 256-PAM, our current prototype utilizes only 4-PAM and 8-PAM. This mainly stems from the low sample rate of the receivers, i.e., 44.1 kHz for audio interface. Therefore, one immediate solution to scale up the data rate is to increase the receiver sample rate. For example, the audio interface of Samsung Galaxy S9 can support up to 384 kHz [29], and latest proposals like PurpleVLC [30] and SmartVLC [31] have adopted an MSps-level ADC (albeit not available to COTS devices yet) to sample 200 kHz OOK transmissions. Moreover, a receiver with a good front-end design, i.e., with an amplifier, may improve the performance of SynLight in terms of both data rate and communication distance, and we may indeed harvest energy from the audio jack (similar to [24]) to power the amplifier. Finally, demodulation on receiver side also play a crucial role impacting throughput. Our current implementation of SynLight receiver mostly relies on straightforward demodulation techniques to independently detect each symbol, so further enhancement can be achieved by a sequence detector.

Transmitter: In order to achieve a balanced complexity between transmitter and receiver, the transmitter needs to be upgraded accordingly. Increasing the transmission frequency beyond 100 kHz can be readily achieved by replacing transistors with MOSFETs, but such a straightforward improvement would demand a drastic increase in receiver sample rate, making the design even more unbalanced. To make a breakthrough, we need to leverage the direct digital-analog conversion ability of our transmitter, i.e., it converts the digital control signal to analog light intensity. Essentially, we may apply OFDM instead of PAM, and use the OFDM's IDFT output to directly drive the SynLight transmitter. As each OFDM subcarrier has a much narrower bandwidth, OFDM is much more robust against intersymbol interference due to the limited modulation bandwidth of COTS LEDs. This is probably the most efficient way to push VLC throughput to Mbps level in practice.

VI. Conclusion

Aiming to bridge the performance gap between practical VLC systems and existing experimental setups, we have designed and presented SynLight in this paper. SynLight is a practical yet novel VLC system built purely upon COTS devices; it achieves a throughput up to 60 kbps. Essentially, SynLight relies on synthetic light emission to generate high-order modulations after eliminating the nonlinear effect of LEDs. Our compact circuit design for SynLight LED transmitter is able to generate high-order PAM symbols with only On-Off controls. Moreover, to handle LED diversity in massive circuit productions, we have also invented an adaptive calibration scheme to automatically adjust light intensity for each PAM symbol. To get immediately usable VLC receivers for mobile devices, we have proceeded to directly interface a PD with a smartphone via its audio jack. To suppress the AC coupling caused by the audio jack for achieving a high throughput, we have further proposed a delicate coding/decoding scheme. Using the SynLight prototype, we have demonstrated the practicality and promising performance of SynLight through extensive experiments.

Our strenuous design process along with the experiment evaluations has provided us with the firsthand knowledge about the potentials and limits of practical VLC systems, as discussed in Section V-D. Based on some of these findings, we are on the way to improve our SynLight prototype: on one hand, adopting a more effective modulation scheme may further boost the data rate, and on the other hand, speeding up the sampling rate might be achieved by, for example, exploiting smartphone add-on modules like Moto-Mods [32].

References

[1] X. Huang, Z. Wang, J. Shi, Y. Wang, and N. Chi, "1.6 Gbit/s Phosphorescent White LED based VLC Transmission Using A Cascaded Pre-Equalization Circuit and A Differential Outputs PIN Receiver," *OSA Opt. Express*, vol. 23, no. 17, pp. 22 034–22 042, 2015.

[2] B. Weir, "Driving The 21st Century's Lights," *IEEE Spectrum*, vol. 49, no. 3, 2012.

[3] C.-L. Chan, H.-M. Tsai, and K. C.-J. Lin, "POLI: Long-Range Visible Light Communications Using Polarized Light Intensity Modulation," in *Proc. of the 15th ACM MobiSys*, 2017, pp. 109–120.

[4] C.-W. Chow, C.-Y. Chen, and S.-H. Chen, "Visible Light Communication Using Mobile-Phone Camera with Data Rate Higher Than Frame Rate," *OSA Opt. Express*, vol. 23, no. 20, pp. 26 080–26 085, 2015.

[5] Y. Yang, J. Nie, and J. Luo, "ReflexCode: Coding with Superposed Reflection Light for LED-Camera Communication," in *Proc. of the 23rd ACM MobiCom*, 2017, pp. 193–205.

[6] H. Elgala, R. Mesleh, and H. Haas, "An LED Model for Intensity-Modulated Optical Communication Systems," *IEEE Photon. Technol. Lett.*, vol. 22, no. 11, pp. 835–837, 2010.

[7] K. Ying, Z. Yu, R. J. Baxley, H. Qian, G.-K. Chang, and G. T. Zhou, "Nonlinear Distortion Mitigation in Visible Light Communications," *IEEE Wireless Commun.*, vol. 22, no. 2, pp. 36–45, 2015.

[8] H. Elgala, R. Mesleh, and H. Haas, "Non-Linearity Effects and Predistortion in Optical OFDM Wireless Transmission Using LEDs," *Inderscience International Journal of Ultra Wideband Communications and Systems*, vol. 1, no. 2, pp. 143–150, 2009.

[9] H. Qian, S. Yao, S. Cai, and T. Zhou, "Adaptive Postdistortion for Nonlinear LEDs in Visible Light Communications," *IEEE Photon. J.*, vol. 6, no. 4, pp. 1–8, 2014.

[10] J. Hao, Y. Yang, and J. Luo, "CeilingCast: Energy Efficient and Location-bound Broadcast through LED-Camera Communication," in *Proc. of the 35th IEEE INFOCOM*, 2016, pp. 1–9.

[11] Z. Tian, K. Wright, and X. Zhou, "The DarkLight Rises: Visible Light Communication in the Dark," in *Proc. of the 22nd ACM MobiCom*, 2016, pp. 2–15.

[12] B. Fahs, M. Romanowicz, and M. M. Hella, "A Gbps Building-to-Building VLC Link Using Standard CMOS Avalanche Photodiodes," *IEEE Photon. J.*, vol. 9, no. 6, pp. 1–9, 2017.

[13] Y. Yang, J. Hao, and J. Luo, "CeilingTalk: Lightweight Indoor Broadcast Through LED-Camera Communication," *IEEE Transactions on Mobile Computing*, vol. PP, no. 99, pp. 1–1, 2017.

[14] C. Danakis, M. Afgani, G. Povey, I. Underwood, and H. Haas, "Using a CMOS Camera Sensor for Visible Light Communication," in *2012 IEEE Globecom Workshops*, 2012, pp. 1244–1248.

[15] P. Hu, P. H. Pathak, X. Feng, H. Fu, and P. Mohapatra, "Colorbars: Increasing Data Rate of LED-to-Camera Communication Using Color Shift Keying," in *Proc. of the 11th ACM CoNEXT*, 2015, pp. 12:1–12:13.

[16] H. Lee, H. Lin, Y. L. Wei, H. I. Wu, H. M. Tsai, and K. Lin, "RollingLight: Enabling Line-of-Sight Light-to-Camera Communications," in *Proc. of 13th ACM MobiSys*, 2015, pp. 167–180.

[17] P. Luo and *et al.*, "Undersampled-Based Modulation Schemes for Optical Camera Communications," *IEEE Communications Magazine*, vol. 56, no. 2, pp. 204–212, 2018.

[18] Y. Yang and J. Luo, "Boosting the Throughput of LED-Camera VLC via Composite Light Emission," in *Proc. of the 37th IEEE INFOCOM*, 2018, pp. 315–323.

[19] D. Tsonev, H. Chun, S. Rajbhandari, J. J. McKendry, S. Videv, E. Gu, M. Haji, S. Watson, A. E. Kelly, G. Faulkner *et al.*, "A 3-Gb/s single-LED OFDM-based Wireless VLC Link Using a Gallium Nitride μLED," *IEEE Photon. Technol. Lett.*, vol. 26, no. 7, pp. 637–640, 2014.

[20] T. Fath, C. Heller, and H. Haas, "Optical Wireless Transmitter Employing Discrete Power Level Stepping," *J. Lightw. Technol.*, vol. 31, no. 11, pp. 1734–1743, 2013.

[21] J. Li, Z. Huang, R. Zhang, F. Zeng, M. Jiang, and Y. Ji, "Superposed Pulse Amplitude Modulation for Visible Light Communication," *OSA Opt. Express*, vol. 21, no. 25, pp. 31 006–31 011, 2013.

[22] C.-H. Yeh, Y.-L. Liu, and C.-W. Chow, "Real-Time White-Light Phosphor-LED Visible Light Communication (VLC) with Compact Size," *OSA Opt. Express*, vol. 21, no. 22, pp. 26 192–26 197, 2013.

[23] S. Schmid, D. Schwyn, K. Aksit, G. Corbellini, T. R. Gross, and S. Mangold, "From Sound to Sight: Using Audio Processing to Enable Visible Light Communication," in *2014 IEEE Globecom Workshops*, 2014, pp. 518–523.

[24] S. Verma, A. Robinson, and P. Dutta, "AudioDAQ: Turning the Mobile Phone's Ubiquitous Headset Port into a Universal Data Acquisition Interface," in *Proc. of the 10th ACM SenSys*, 2012, pp. 197–210.

[25] L. Li, P. Hu, C. Peng, G. Shen, and F. Zhao, "Epsilon: A Visible Light Based Positioning System," in *Proc. of 11th USENIX/ACM NSDI*, 2014, pp. 331–343.

[26] T. Komine and M. Nakagawa, "Fundamental Analysis for Visible-Light Communication System Using LED Lights," *IEEE Trans. Consum. Electron.*, vol. 50, no. 1, pp. 100–107, 2004.

[27] "PDA36A-EC - Si Switchable Gain Detector," https://www.thorlabs.com/thorproduct.cfm?partnumber=PDA36A-EC.

[28] S. Rajagopal, R. Roberts, and S. Lim, "IEEE 802.15.7 Visible Light Communication: Modulation Schemes and Dimming Support," *IEEE Commun. Mag.*, vol. 50, no. 3, pp. 72–82, 2012.

[29] "Samsung Galaxy S9," https://www.gsmarena.com/samsung_galaxy_s9-8966.php.

[30] S. Yin, N. Smaoui, M. Heydariaan, and O. Gnawali, "Purple VLC: Accelerating Visible Light Communication in Room Area through PRU Offloading," in *Proc. of the 15th EWSN*, 2018, pp. 67–78.

[31] H. Wu, Q. Wang, J. Xiong, and M. Zuniga, "SmartVLC: When Smart Lighting Meets VLC," in *Proc. of the 13th ACM CoNEXT*, 2017, pp. 212–223.

[32] "Motorola Moto Mods," https://www.motorola.com/us/moto-mods.